Research Journal of Applied Sciences, Engineering and Technology 6(2): 249-253, 2013
DOI:10.19026/rjaset.6.4065
ISSN: 2040-7459; e-ISSN: 2040-7467

Submitted: December 17, 2012 Accepted: February 01, 2013 Published: June 10, 2013

Research Article

Analysis of Pre-Blasting Cracks in Horizontal Section Top-coal Mechanized Caving of Steep Thick Seams

[1]Shu-Ren Wang, [2, 3]Xing-Ping Lai and [2, 3]Peng-Fei Shan
[1]School of Civil Engineering and Mechanics, Yanshan University, Qinhuangdao, China
[2]School of Energy Engineering, Xi'an University of Science and Technology, Xi'an, China
[3]Key Laboratory of Western Mine and Hazard Prevention, Ministry of Education, Xi'an, China

Abstract: In order to achieving safe and efficient exploitation in horizontal section top-coal mechanized caving of steep and thick seams, pre-blasting of top-coal is one of the prerequisites and analysis of crack evolution law is a key method to achieving good pre-splitting effects. Based on investigations of coal seams and mining conditions, theories of fracture mechanics were applied to explain the process of caving cracks and fracture toughness of coal seams in pre-blasting caving were calculated. The distribution of caving cracks was determined with in-situ borehole-wall real deformation optical monitoring systems. The results showed that the pre-splitting crack could rapidly develop in the direction of borehole center line and form the failure surface along the same direction in the last; the fracture toughness of B_3 and B_6 coal seams was 0.5616 and 1.1900 $MPa \cdot m^{1/2}$, respectively. The distribution of caving stress from real monitoring instruments provided a theoretical proof for optimizing the parameters of pre-blasting in top-coal safe mining.

Keywords: Fracture toughness, pre-blasting, steep thick seam, top-coal mechanized caving

INTRODUCTION

Mechanized Top-Coal Caving Technology (MTCCT) has a long history. From the early 1950s, MTCCT has been applied in countries such as the former Soviet Union, France, Poland, Yugoslavia and India. However, less than ideal results, foreign MTCCT began to shrink in the late 1980s (Oosthuizen and Esterhuizen, 1997; Zhang and Qian, 2003; Vakili and Hebblewhite, 2010).

In China, a series of tests on MTCCT had been conducted in Shenyang, Pingdingshan, Lu'an and Yangquan Mining Bureau since 1982 and after a number of technical setbacks, the thick coal seam caving efficiency and security issues were satisfactorily solved in the late 1980s, which promoted the technology to develop rapidly and now it has become a main method of thick seam mining in China (Xie *et al*., 1999; Ren, 2005; Wang *et al*., 2006; Liu *et al*., 2009).

Pre-blasting in top-coal caving is one of the prerequisites to achieving efficient and safe mining. Specifically, to transform top coal from the original state to caving state, three phases of complex processes are required, namely deformation, broken inflation and falling. Crack evaluation law analysis is a crucial method to achieve pre-blasting and weaken coal in steep and thick seams, which includes top-coal sturdiness coefficient testing, scope of loose top-coal, advanced stress influence, blasting parameters, equipment supporting, caving distance and coal spontaneous combustion in mined-out areas, determination of support method after pre-blasting, considering hole parameters, packaging quality, minimal resistance line, the interaction between caving in front of hydraulic mechanized support with initiation sequence, drilling angle and length in pre-blasting (T.H. Kang *et al*., 2004; Yasitli and Unver, 2005; Unver and Yasitli, 2006; Encina *et al*., 2010).

According to an investigation of the geological and mining conditions, based on +564 m B_{3-6} in Jiangou Coal Mine, China, in order to obtain good pre-splitting effects and to ensure safe mining, optimization parameters of the crack expanding processes in pre-blasting were achieved by fracture mechanics and in-situ stress monitoring

ENGINEERING SITUATION

Engineering geological environment and mining conditions: Pre-blasting lanes, +564 m B_{3-6} coal seams, Jiangou Coal Mine, are layed out along strike and the center distance between lanes is 45.0 m. The total coal thickness is 50.0 m and its average angle is 86.5°. The methane levels are low, but there is still a hazard of coal dust explosion. The coal has a propensity for spontaneous combustion. Table 1 lists characteristics of roof and floor geological conditions.

Correspondong Author: Shu-Ren Wang, School of Civil Engineering and Mechanics, Yanshan University, Qinhuangdao, China, Tel.: 13273373298

Table 1: Physical and mechanical parameters of rock mass.

Lithology name	Lithologics	Density (kg/m^3)	Lithological traits
Main roof	Shale	2380	Hard, dark grey, layer structure
Immediate roof	Siltstones	1440	Grey, layer structure, joint well
False roof	Shale	2450	Soft, joint obvious
Immediate floor	Shale	2600	Joint obvious, fragile

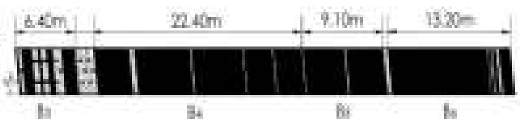

Fig. 1: Geological section condition and thickness of B3-6 coal seams

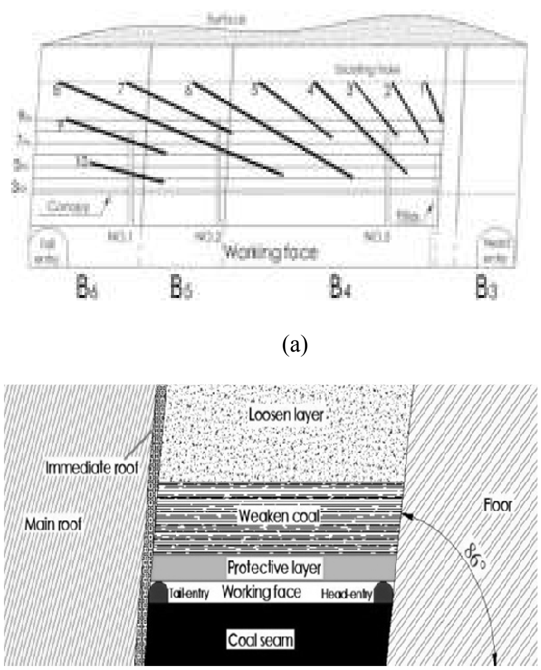

(a)

(b)

Fig. 2: Pre-blasting plan boreholes and working face; (a) Profile of pre-blasting plan boreholes; (b) Physics model of working face during advancing

As shown in Fig. 1, the seam thickness ranges from B_6 to B_3 respectively, four partings lie in B_4-B_5 and the thickness of parting is between 0.15 and 0.20 m, thus, average thickness is 0.16 m.

Based on existing technologies and on-site hazard identification, a pre-blasting program was developed as follows:

In the top-coal, there were groups of blasting holes (fan-shaped, one-way vertical seams, diameter: 100 mm, blast-hole spacing: 4.0 m, 10 boreholes in each group) were arranged from B_3 to B_6 Lane. Pre-blasting was conducted to weaken the top-coal by latex matrix explosives. The protection or safe thickness of top-coal should be 3.0 m, with 5.0 m width of coal pillar, using Charge Machine and yellow mud sealing.

Plan of monitoring points' position: As shown in Fig. 2, No. 1-3 monitoring boreholes were located at 3.5 m high from the scraper bottom to top-coal seam, with 2.8 m away from No. 53 group borehole (Hole 3, hole 6 and hole 9) and 1.2 m from No. 53 group mined-borehole (Hole 1, hole 4, hole 7 and hole 10) and 1.2 m from No. 53 group middle borehole (Hole 2, hole 5 and hole 8). Both No. 1 and No. 3 monitoring boreholes are 8 m deep and that of No. 2 monitoring borehole is 9 m. Furthermore, No. 1 monitoring borehole lies in B_4 seam, 1.2 m away from No. 53 group and is intersect with hole 4 at 5.0-6.0 m. No. 2 monitoring borehole lies in B_5 seam, 1.2 m away from No. 53 group. No. 3 monitoring borehole lies in B_6 seam, 1.2 m away from No. 53 group and is intersect with hole 10 at 3.0-5.0 m.

EXPERIMENTAL METHODS

In-situ real deformation monitoring: In situ borehole-wall optical systems were applied to observe crack degrees and the distribution of crack network. This information is gathered by scopes of testing devices to reveal the top-coal rupture characteristics and rules. The high-resolution probes and color display device were adopted to conduct in-situ real deformation monitoring, which can distinguish cracks correct to 1 mm. The computer can be connected directly to facilitate real-time image display and preservation, as shown in Fig. 3.

Calculation method of fracture toughness: After the pre-blasting borehole in the top-coal, blast stress wave in the wave-front surface generates a radial compressive stress and circumferential tensile stress, which causes a dynamic stress concentration at the borehole-wall along the borehole center line. As a result, the initial fracture can be prior formed by the tensile stress along the borehole center line direction. Under the quasi-static stress field of the detonation gases, the pre-splitting borehole will produce the stress concentration area of the initial crack tip, leading to further expansion of the initial cracks (Zong, 1998).

As shown in Fig. 4. The process of crack expansion can be analyzed by a computational model of fracture mechanics and the crack can be simplified in the plane strain state.

In Fig. 1a, due to the velocity that static gases get into the crack is less than that of the crack expansion and the static gases effects in the cracks can be ignored. So Eq. 1 can be used to describe stress intensity factor at the crack tip:

$$K_{\mathrm{I}} = f \cdot P_{\mathrm{qs}} (\pi \cdot a_{\mathrm{s}})^{\frac{1}{2}} \tag{1}$$

where,

K_{I} = Rock stress intensity factor

P_{qs} = Quasi-static pressure of the borehole

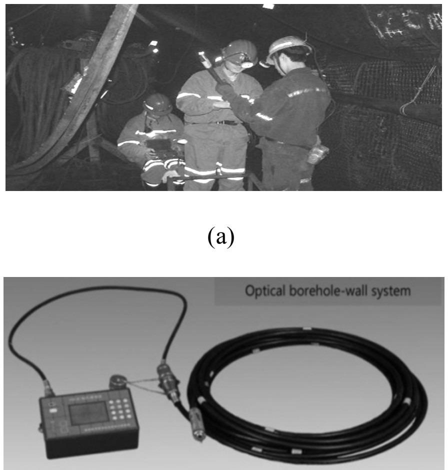

(a)

(b)

Fig. 3: In situ monitoring pictures: (a): Monitoring workers; (b): Monitoring instruments

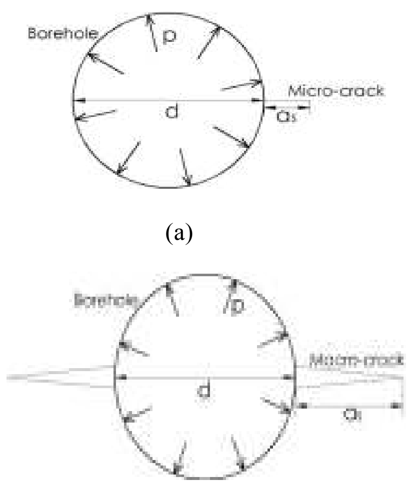

(a)

(b)

Fig. 4: The computational model: (a): Before fracture; (b): After fracture

a_s = Length of radial extension
f = Correction factor related with a_s and diameter d of the borehole

For the initial crack extension, it must satisfy Eq. 2:

$$K_I > K_{Ic} \tag{2}$$

where, k_{Ic} is rock fracture toughness.

When the crack extension length of the borehole is much longer than the radius, the calculation can be simplified by Fig. 2b. Then Eq. 3 can be used to describe the stress intensity factor of the crack tip stress field.

Under such condition, Eq. 3 could describe stress intensity factors at the crack tip:

$$K_1 = d \cdot P_{qs} (\pi \cdot a_1)^{\frac{1}{2}} \tag{3}$$

where,
a_1 = The final length of crack
d = Diameter of the borehole

According to fracture mechanics, the longer length of the initial crack, the easier it is to be developed. Hence, the crack will quickly expand to form the rupture surface along the borehole center line.

After emulsion matrix's detonation**,** the average explosive pressure can be described as:

$$P_m = \frac{1}{8} \rho_0 D^2 \tag{4}$$

where,
P_m = Average explosive pressure
ρ_0 = Density of emulsion matrix
D = Velocity of emulsion matrix

According to the calculation, the outcome is 2025-3164 MPa. In addition, the equation of quasi-static pressure of the hole can be described as:

$$P_{qs} = \left(\frac{P_m}{P_k}\right)^{\frac{k}{n}} \cdot \left(\frac{d_c}{d}\right)^{2k} \cdot P_k \tag{5}$$

where,
P_k = Critical pressure of explosive gas in expansion process, is 100 MPa
d_c = Diameter of dynamite
n = A constant 3
k = The adiabatic coefficient 1.3-1.4

The calculated quasi-static pressure is 10.02-10.36 Mpa.

RESULTS AND DISCUSSION

Borehole deformation analysis: From all above mentioned, it is possible for us to observe various cracks in the No. 1-3 monitoring boreholes. Figure 5 exhibits partial ones collected from field boreholes information, which presents crack degrees and the distribution of fracture network.

Statistics analysis of these cracks in each borehole were shown in Fig. 6. Above all, analysis of in-situ real deformation monitoring can be achieved:

- Monitoring borehole was located at B_4 coal (softer) and was influenced largely by hole 4 blasting. Cracks developed apparently from 0 to 1.0 m, with vertical crack densely between 1.0 to 2.5 m, with a maximum of 4.5 m. Due to the blasting effects, the bore-hole with broken free surface, it had the crushed loose coal. Some cracks developed at a depth of around 2.5 m, which may cause roof caving.

(a)

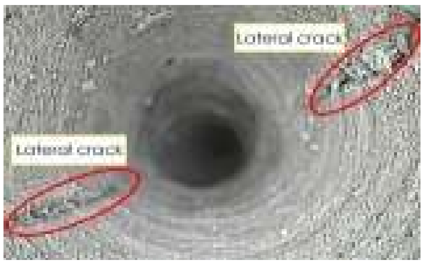

(b)

(c)

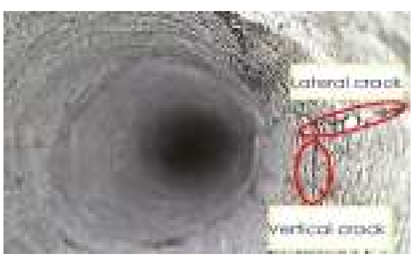

(d)

Fig. 5: All kinds of borehole cracks (a): Oblique crack; (b): Lateral crack; (c): Circular crack; (d): Lateral crack and vertical crack

- Monitoring borehole was located at B_5 coal (Which was harder than B_4) and hole 7 intersects with No. monitoring 2 borehole at 7.0-9.0 m. Cracks are mainly focused on about 1.0 m and there was some broken coal from 5.5 to 6.5 m. Overall, the inner wall of No. 2 monitoring borehole maintained integrity.
- Monitoring borehole was located at B_6 coal and was affected by hole 10 blasting. This monitoring borehole had dual circular cracks from 0 to 1.0 m, with broken section scattered between 0 to 3.0 m.

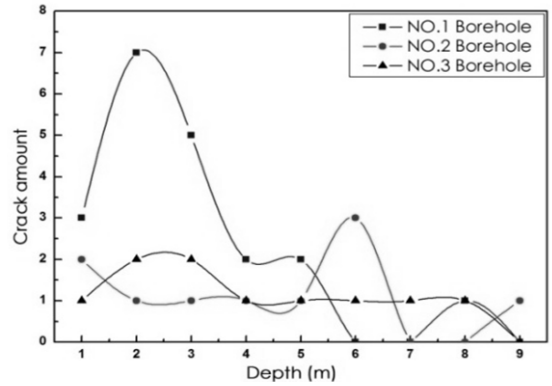

Fig. 6: Statistical regularity of cracks with advent of borehole depth

Table 2: Parameters of emulsion matrix

Density (g/cm^3)	Velocity (m/s)	Loose zone (m)	Diameter (mm)	Efficiency (%)
1.25	3600-4500	6	25	96-100

Table 3: Parameters of cracks in boreholes

Position	Borehole	Angel (°)	Width (mm)	Length (mm)	Fracture toughness ($MPa \cdot m^{1/2}$)
B_4	1#	90	1-3	100-230	0.5616-0.8806
B_5	2#	90	2-4	130-270	0.6403-0.9541
B_6	3#	90	3-5	180-420	0.7535-1.1900

Calculation of fracture toughness: After pre-blasting being completed, a large amount of free surfaces brought about lamination crack phenomenon by blasting stress waves in No. 1-3 monitoring boreholes, which caused cracks to grow and develop well. Details of emulsion matrix can be seen from Table 2.

Parameters of cracks in No. 1-3 monitoring boreholes were listed in Table 3. Because average length of crack was distinctly more than radius of holes, Eq. 3 was adopted for computing the fracture toughness and the results can be seen from Table 3.

Pre-blasting stress monitoring: As shown in Fig. 7, the instruments were applied for the stress monitoring. On one side, it can be (a) From the working face, abutment pressure is not obvious from 0 to 10.0 m. (b) From 10.0 to 15.0 m, the pressure was 0.2-1.0 MPa and kept steady. Because of pre-blasting, abutment pressure rose suddenly to 2.5 MPa and then lessened a little towarded a new balance. On the other side, roof load at stope varied rarely in the explosive process:

- From 0 to 8.0 m, the roof load went up gradually and its peak added up to 2.5 MPa.
- Based on results of the stress monitoring, 4.0 m roof canopy is used to control caving and sliding above
- From 8.0 to 13.0 m, roof load increased sharply by fluctuating stress and its peak added up to 3.5 MPa and then also lessened a little towards another new balance.

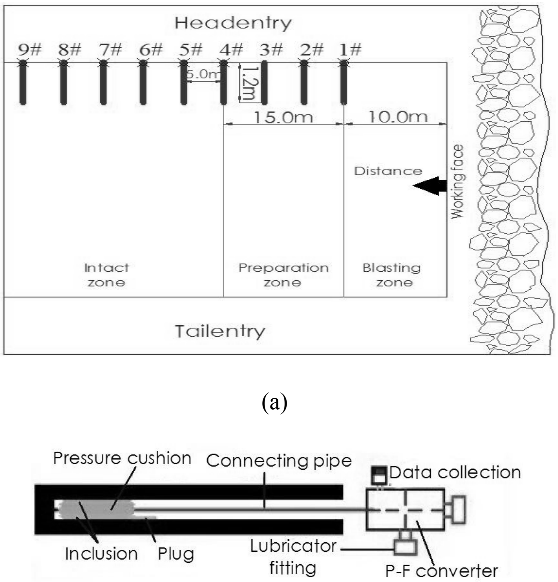

(b)

Fig. 7: In-situ monitoring conditions; (a): Layout of general in-situ monitoring; (b): Stress monitoring principle and field data acquisition

Based on results of the stress monitoring, 4.0 m roof canopy is used to control caving and sliding above supports. Advanced supporting from 0 to 45.0 m is identical to the field situation.

CONCLUSION

After pre-blasting in steep and thick seam, as explosive effects cause dynamic stress focusing on pore wall along the central line, so initial cracks form along the central line, then under the quasi- static stress from explosive gases, initial cracks grows further.

The average length of crack is much more than the radius of holes, the fracture toughness of B_3 and B_6 coal seams was 0.5616 and 1.1900 $MPa \cdot m^{1/2}$, respectively which has been used to optimize parameters of pre-blasting.

In-situ real monitoring results show that mining pressure is not fierce and its peak decreases obviously, abutment pressure moves toward working face and stress concentration zone lessens apparently.

ACKNOWLEDGMENT

This study was financially supported by the National Natural Science Foundation of China (51074140, 11002021), the China Scholarship Council (CSC) & the Hebei Provincial Office of Education (2010813124), the Doctoral Subject Foundation of the Ministry of Education of China (20070008012) and the National High Technology Research and Development Program (2008AA062104), all these are gratefully acknowleged.

REFERENCES

Encina, V., D. Méndez, C. Caballero and H. Osorio, 2010. New approach for rapid preparation of block caving mines. Transactions of the Institutions of Mining and Metallurgy, Section A: Mining Technology, 119(3): 162–167.

Kang, T.H., J.P. Zhang and S.W. Bai, (2004). Theoretical study and application of weakening top coal using water pre-infusion in fully mechaninized sublevel caving mining. Chinese J. Rock Mech. Eng., 23(15): 2615-2617, (In Chinese).

Liu, C.Y., B.X. Huang and F.F. Wu, 2009. Technical parameters of drawing and coal-gangue field movements of a fully mechanized large mining height top coal caving working face. Min. Sci. Technol. China, 19(5): 549-555.

Oosthuizen, J.B. and G.S. Esterhuizen, 1997. Evaluation of three rock breaker layouts for mechanized block cave mining. J. S. Afr. I. Min. Metall., 97(6): 269-273.

Ren, R.H., 2005. Surface movement regularity of super-wide mining face with top-coal caving. J. China Univ. Min. Technol., 15(1): 68-71.

Unver, B. and N.E. Yasitli, 2006. Modelling of strata movement with a special reference to caving mechanism in thick seam coal mining. Int. J. Coal Geol., 66(4): 227-252.

Vakili, A. and B.K. Hebblewhite, 2010. A new cavability assessment criterion for Long wall top coal caving. Int. J. Rock Mech. Min., 47(8): 1317-1329.

Wang, S.R., J.A. Wang, S.H. Liu, S.C. Wu and J.W. Xie, 2006. Distinct element analysis on the rules of coal movement and the failure mechanism due to mechanized top-coal caving in steep thick seam. J. Univ. Sci. Technol. Beijing, 28(9): 802-812, (In Chinese).

Xie, H.P., Z.H. Chen and J.C. Wang, 1999. Three-dimensional numerical analysis of deformation and failure during top coal caving. Int. J. Rock Mech. Min., 36(5): 651-658.

Yasitli, N.E. and B. Unver, 2005. 3-D numerical modelling of stresses around a long wall panel with top coal caving. J. S. Afr. I. Min. Metall., 105(5): 287-300.

Zhang, X.C. and M.G. Qian, 2003. China's Coal Mining Science and Technology. China Coal Industry Publishing House, Beijing, (In Chinese).

Zong, Q., 1998. Investigations into mechanism of crack formation for grooved hole well blasting. Chinese J. Geotech. Eng., 20(1): 30-33, (In Chinese).